Neuron, Vol. 40, 749–762, November 13, 2003, Copyright ©2003 by Cell Press

Endophilin Is Required for Synaptic Vesicle Endocytosis by Localizing Synaptojanin

Kimberly R. Schuske,[1] Janet E. Richmond,[2,4] Dawn Signor Matthies,[1,4,5] Warren S. Davis,[1] Steffen Runz,[1] Daniel A. Rube,[3] Alexander M. van der Bliek,[3] and Erik M. Jorgensen[1,*]
[1]Department of Biology
University of Utah
257 South 1400 East
Salt Lake City, Utah 84112
[2]Department of Biological Sciences
University of Illinois at Chicago
Chicago, Illinois 606067
[3]Department of Biological Chemistry
University of California at Los Angeles School of Medicine
Los Angeles, California 90095

Summary

Endophilin is a membrane-associated protein required for endocytosis of synaptic vesicles. Two models have been proposed for endophilin: that it alters lipid composition in order to shape membranes during endocytosis, or that it binds the polyphosphoinositide phosphatase synaptojanin and recruits this phosphatase to membranes. In this study, we demonstrate that the *unc-57* gene encodes the *Caenorhabditis elegans* ortholog of endophilin A. We demonstrate that endophilin is required in *C. elegans* for synaptic vesicle recycling. Furthermore, the defects observed in endophilin mutants closely resemble those observed in synaptojanin mutants. The electrophysiological phenotype of endophilin and synaptojanin double mutants are virtually identical to the single mutants, demonstrating that endophilin and synaptojanin function in the same pathway. Finally, endophilin is required to stabilize expression of synaptojanin at the synapse. These data suggest that endophilin is an adaptor protein required to localize and stabilize synaptojanin at membranes during synaptic vesicle recycling.

Introduction

To maintain neurotransmitter release during stimulation, synaptic vesicles must be recycled after they fuse with the plasma membrane. The best-characterized mechanism for synaptic vesicle recycling is through clathrin-mediated endocytosis. There are four main steps to clathrin-mediated endocytosis: recruitment, budding, fission, and vesicle uncoating (De Camilli et al., 2000; Harris et al., 2001). In the first step, vesicle proteins, clathrin adaptor proteins, and clathrin are recruited to the site where endocytosis will occur. Second, the assembled clathrin matrix causes the membrane to invaginate or bud into the cytoplasm of the neuron. This early shallow pit is converted into a deeply invaginated pit, possibly by a change in membrane composition at the base of the invaginating bud (Schmidt et al., 1999). Third, fission separates the budded vesicle from the plasma membrane. Fourth, the clathrin coat is removed from the internalized vesicle. The key molecular components of this pathway are clathrin and the adaptor complex, which are required for budding, and dynamin, which participates in cleaving the budded vesicle from the plasma membrane. A large number of interacting proteins that are localized to synapses and bind these components have been identified by biochemical methods (Slepnev and De Camilli, 2000). However, it is not clear how these accessory factors function during endocytosis.

One of these accessory proteins is endophilin (Ringstad et al., 1997). The amino terminus of endophilin A contains a domain that mediates dimerization and lipid binding (Farsad et al., 2001; Ringstad et al., 2001; Schmidt et al., 1999), and the carboxyl terminus contains an SH3 domain that binds amphiphysin and the proline-rich domains of dynamin and synaptojanin (de Heuvel et al., 1997; Micheva et al., 1997b; Modregger et al., 2003; Ringstad et al., 1997). Endophilin was originally identified as a binding partner for synaptojanin, a phosphatidylinositol phosphatase required for synaptic vesicle recycling (Ringstad et al., 1997). Since its discovery, several studies on endophilin have indicated that endophilin functions during synaptic vesicle recycling (Farsad et al., 2001; Guichet et al., 2002; Hill et al., 2001; Ringstad et al., 1999; Schmidt et al., 1999; Simpson et al., 1999; Tang et al., 1999; Verstreken et al., 2002). These studies have led to the advancement of two main hypotheses for endophilin function.

First, endophilin may alter the membrane composition at the base of the invaginating bud to promote the conversion of shallow invaginating coated pits into deeply invaginated pits (Farsad et al., 2001; Ringstad et al., 1999; Schmidt et al., 1999). This model arises from the observed enzymatic activity of endophilin: the protein can condense lysophosphatidic acid and acyl-CoA into phosphatidic acid (Schmidt et al., 1999). The cone shape of phosphatidic acid is more compatible with a high index of curvature than the inverted cone shape of lysophosphatidic acid and thus might drive the shallow bud into a deeply invaginated pit. Disruption of endophilin function by injection of antibodies against the SH3 domain into the lamprey giant synapse causes an accumulation of shallow and deeply invaginated coated pits (Ringstad et al., 1999). In addition, accumulation of membrane ruffles and shallow pits are observed in *Drosophila* endophilin mutants (Guichet et al., 2002; Verstreken et al., 2002). These studies lend support to the model that endophilin is required for the late budding stage of endocytosis.

Second, endophilin has been proposed to act as an adaptor protein. The SH3 domain of endophilin binds the proline-rich domains of synaptojanin and dynamin

*Correspondence: jorgensen@biology.utah.edu
[4]These authors contributed equally to this work.
[5]Present address: Department of Pharmacology, Vanderbilt University, Nashville, Tennessee 84112.

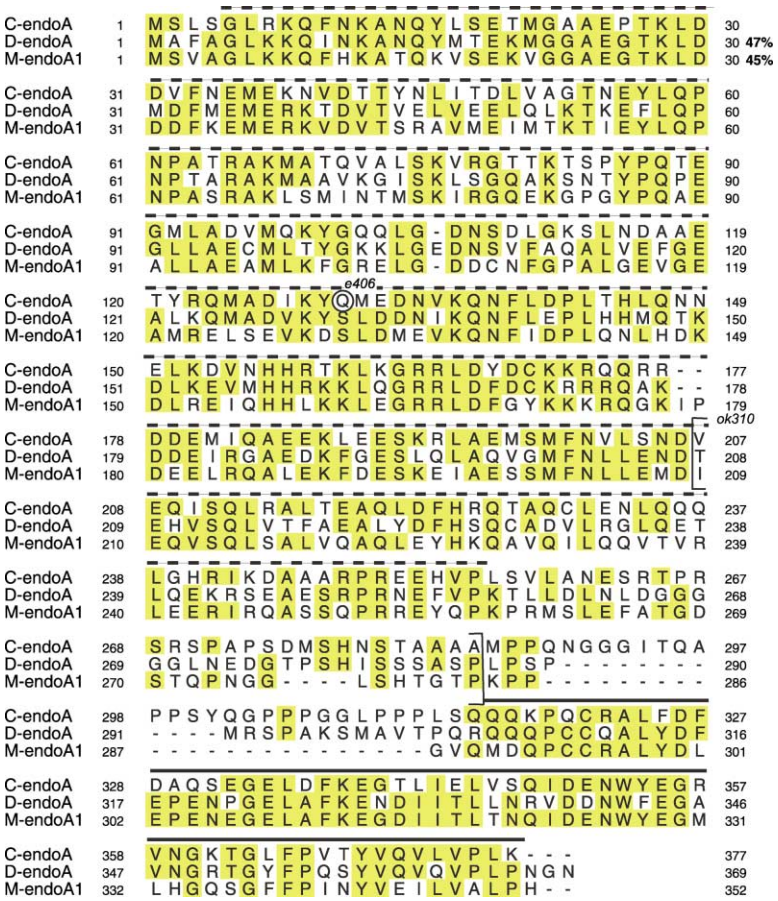

Figure 1. Sequence Alignment between *C. elegans*, *Drosophila*, and Mouse Endophilin A Proteins

Mouse endophilin A1 (accession # U58886) and *Drosophila* endophilin A (accession # AF426170) were used as the query in Blast searches; the *C. elegans* ORF T04D1.3 has the highest-scoring identity in the worm genome. The alignment shown uses a corrected version of *C. elegans* endophilin A, which was determined by sequencing the yk1305d cDNA (AY394006). Sequence alignments were made using Clustal X and Seq View. Dashed bar designates the BAR domain/LPAAT activity. Solid bar designates sequence corresponding to the SH3 domain. The *unc-57(e406)* glutamine (Q) to stop mutation is indicated. The residues removed in the *unc-57(ok310)* deletion are shown in brackets.

and may be required to recruit these proteins to the sites where they function during endocytosis (Ringstad et al., 1997). Dynamin is a GTPase that is required to cleave the vesicle from the plasma membrane. A temperature-sensitive mutation in the *Drosophila shibire* gene, which encodes dynamin, causes an accumulation of deeply invaginated coated pits at the plasma membrane (Koenig and Ikeda, 1989). In addition, transfection of the SH3 domain of endophilin in cell culture or injection of this domain into the lamprey giant synapse causes an accumulation of deeply invaginated pits, suggesting that this domain might be blocking dynamin function (Gad et al., 2000; Simpson et al., 1999). Analysis of synaptojanin mutants demonstrates that this lipid phosphatase is required for multiple steps of endocytosis (Cremona et al., 1999; Harris et al., 2000). Synaptojanin mutants in *C. elegans* exhibit a depletion of synaptic vesicles and an increase in the number of deeply invaginated pits and clathrin-coated vesicles at the synapse (Harris et al., 2000). A similar phenotype was observed when peptides or antibodies that specifically block synaptojanin interactions with the endophilin SH3 domain were injected into the lamprey giant synapse (Gad et al., 2000). Together, these data suggest that endophilin binding may be important for synaptojanin function.

To determine the role of endophilin during clathrin-mediated endocytosis, we have characterized *C. elegans* mutants that lack the endophilin protein. We demonstrate that endophilin mutants are defective for synaptic vesicle recycling and that this defect closely resembles the phenotype observed in synaptojanin mutants. Furthermore, the phenotypes associated with a loss of synaptojanin function are not exacerbated by mutations in endophilin. Finally, our data indicate that endophilin is required for synaptojanin stabilization at the synapse. Therefore, our study suggests that the main role for endophilin is as an adaptor molecule for synaptojanin.

Results

Endophilin proteins contain a large BAR domain, an N-terminal coiled-coil domain within the BAR domain, and a C-terminal SH3 domain (Figures 1 and 2; Letunic et al., 2002; Ringstad et al., 1997; Schultz et al., 1998). In vertebrates there are two subfamilies of endophilin proteins, endophilin A and B (Modregger et al., 2003). The A isoform is primarily required for endocytosis at the plasma membrane (Farsad et al., 2001; Guichet et al., 2002; Hill et al., 2001; Ringstad et al., 1999; Schmidt et al., 1999; Simpson et al., 1999; Tang et al., 1999; Verstreken et al., 2002), whereas one B isoform has been shown to be required for trafficking of internal membranes (Modregger et al., 2003). In *C. elegans* there are single genes encoding orthologs for each of these

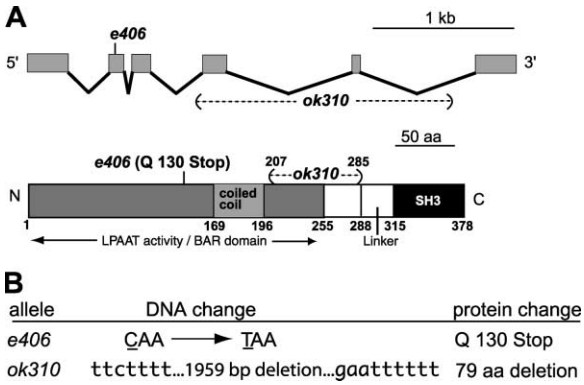

Figure 2. Genomic Location and Structure of the *unc-57* Locus

(A) *unc-57* gene and protein structure. The genomic structure of the rescuing open reading frame T04D1.3 is shown (the corrected version was determined by sequencing the yk1305d cDNA). Protein domain structure is shown below. The BAR domain is found at the amino terminus of endophilin (Letunic et al., 2002; Schultz et al., 1998). This same region confers lysophosphatidic acid acyl transferase activity (Schmidt et al., 1999). The coiled coil domain mediates dimerization (Ringstad et al., 2001). The SH3 domain binds the proline-rich domain of synaptojanin and dynamin (Micheva et al., 1997a; Ringstad et al., 1997).

(B) Alleles. Sequence of mutations in the alleles *unc-57(e406)* and *unc-57(ok310)*. *unc-57(e406)* was generated by EMS. *unc-57(ok310)* was generated by TMP/UV.

protein subfamilies. The *C. elegans* endophilin A ortholog (T04D1.3) is 45% identical to mouse endophilin A1 and 47% identical to *Drosophila* endophilin A (Figure 1), but it is only 20% identical to mouse endophilin B1 and 16% identical to *Drosophila* endophilin B. In *C. elegans* the endophilin B protein, F35A5.8b, is 47% identical to mouse endophilin B1. We characterized the role of *C. elegans* endophilin A in synaptic vesicle endocytosis.

C. elegans endophilin A is encoded by the *unc-57* gene. There are two mutations of the gene, *unc-57(ok310)* and *unc-57(e406)* (Figures 1 and 2). *unc-57(ok310)* is a deletion of 1.9 kb and removes exons four and five. Because the endpoints of the deletion are in introns, it is possible that a truncated protein could be generated that would contain the coiled-coil domain as well as the SH3 domain. However, conserved residues in the BAR domain would be eliminated. The function of the BAR domain is not known but is found in adaptor proteins such amphiphysin, Bin1, and the yeast proteins Rvs167 and Rvs161 (Balguerie et al., 1999; Ge and Prendergast, 2000). Contained within the BAR domain of endophilin are residues required for lipid binding and lysophosphatidic acid transferase activity (Farsad et al., 2001; Schmidt et al., 1999). *unc-57(e406)* is an A to G transition in the second exon of the endophilin locus that changes glutamine 130 into a stop codon. *unc-57(ok310)* and *unc-57(e406)* have identical phenotypes and fail to complement each other; it is presumed that these alleles represent the null phenotype. A genomic fragment that contains the endophilin open reading frame and 2 kb of upstream sequence rescues the uncoordinated phenotype of both *ok310* and *e406*, demonstrating that the uncoordinated phenotype in these strains is caused by the mutations in the endophilin gene.

It has been proposed that endophilin is an adaptor molecule required to localize the endocytic proteins dynamin and synaptojanin to endocytic zones (Ringstad et al., 1997). If the sole role for endophilin is to localize these proteins to sites of endocytosis, then endophilin mutants should have the same phenotype as dynamin or synaptojanin mutants. However, a complete loss of dynamin/*dyn-1* causes an early larval lethal phenotype in *C. elegans* (A.M.v.d.B., data not shown), whereas endophilin/*unc-57* mutants are viable. By contrast, *unc-57* mutant animals have a distinctive uncoordinated behavioral phenotype that is shared by synaptojanin/*unc-26* mutants. Both mutants are small, grow slowly, exhibit jerky backward movements, and tend to coil. In addition, both *unc-57* and *unc-26* animals have the same level of resistance to the drug Aldicarb, an inhibitor of the degradative enzyme for acetylcholine, indicating a comparable decrease in acetylcholine release in the mutants (Figure 7A). Previous work demonstrated that *unc-26* mutants have defects in the endocytosis of synaptic vesicles (Harris et al., 2000); therefore, we sought to determine if endophilin mutants also exhibit similar defects in endocytosis at synapses.

Endophilin Is Localized to Synapses

If endophilin is required for synaptic vesicle recycling, then it should be expressed in neurons and localized to synapses. To determine in which cells endophilin is expressed, 4.5 kb of upstream promoter sequence was used to drive GFP expression. Fluorescence was observed in all neurons and the posterior intestine (Figure 3A). To determine where the endophilin protein is located, GFP was fused to the C terminus of the protein. This construct rescued the *unc-57(ok310)* mutant phenotype, demonstrating that the fusion protein is properly localized. GFP-tagged endophilin was enriched in puncta in all neuropil and colocalized with synaptobrevin, demonstrating that endophilin is localized to synapses (Figure 3B). In addition, weak protein expression was observed in the spermatheca (data not shown). Furthermore, analysis of a genotype that mislocalizes synaptic vesicles suggests that endophilin may be associated with vesicles. The kinesin motor protein, encoded by the *unc-104* gene, is required for synaptic vesicle transport from the cell body to neuromuscular junctions (Hall and Hedgecock, 1991; Jorgensen et al., 1995). In *unc-104* mutants, GFP-tagged endophilin accumulated in the cell bodies rather than at synapses (Figures 3C and 3D). These data suggest that endophilin is a cargo of the synaptic vesicle kinesin. The simplest interpretation of this result is that endophilin is associated with synaptic vesicles. However, it is also possible that endophilin requires synaptic vesicle cycling at the synapse for proper localization and that endophilin mislocalization is an indirect consequence of synaptic vesicle mislocalization in the kinesin mutant.

Endophilin Mutants Exhibit Defects in Synaptic Vesicle Endocytosis

If synaptic vesicle endocytosis is defective in *unc-57* mutants, then synaptic proteins should be mislocalized to the axonal plasma membrane and there should be a reduction of synaptic vesicles at synapses. We assayed

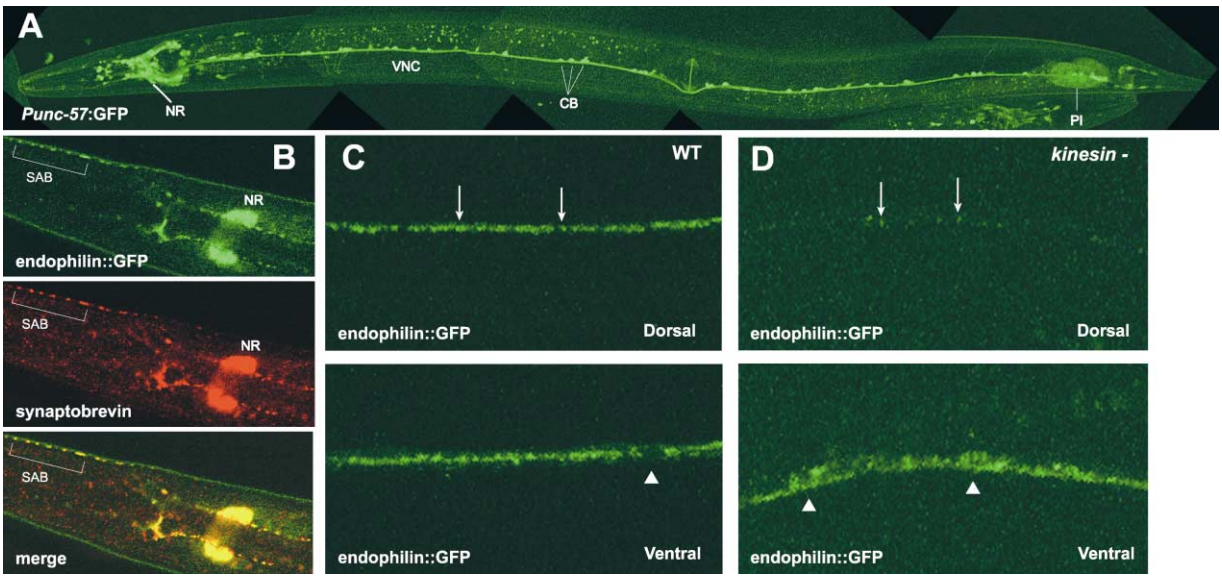

Figure 3. Expression of *C. elegans* Endophilin

(A) Endophilin is expressed in neurons. 4.5 kb of promoter sequence upstream of *unc-57*/T04D1.3 was fused to GFP. A confocal fluorescence micrograph of an adult hermaphrodite is shown. The worm is positioned so that the ventral cord is exposed; the anterior of the worm is left. Expression is observed in all neurons. Abbreviations: NR, nerve ring; VNC, ventral nerve cord; CB, cell bodies; PI, posterior intestine. Neuromuscular junctions are found along the ventral nerve cord.

(B) Endophilin is localized to synapses. Dorsal view of the head of an adult hermaphrodite; anterior is left. Top, GFP-tagged endophilin (green). This tagged construct rescues the *unc-57* phenotype. Bracket: punctate staining is observed at the neuromuscular junctions of the SAB neurons. Bright staining to the right is a cross-section through the nerve ring (NR), the major neuropil in the head. Middle, synaptobrevin immunoreactivity (red) is localized to synaptic regions. Bottom, merged image demonstrates that endophilin-GFP colocalizes with synaptobrevin at synapses. Antibody staining was performed as previously described (Miller and Shakes, 1995).

(C) Endophilin is localized to neuromuscular junctions. A section of the dorsal and ventral nerve cords of a worm expressing GFP-tagged endophilin (genotype, *lin-15(n765ts); oxIs91[*UNC-57-GFP; *lin-15+])*. The ventral and dorsal cords show punctate localization of the GFP-tagged endophilin protein (small arrows), consistent with a localization to neuromuscular junctions. Cell bodies of the motor neurons are only located in the ventral nerve cord (arrowheads).

(D) Endophilin is mislocalized in a kinesin mutant. GFP-tagged endophilin remains in the motor neuron cell bodies in the absence of the synaptic vesicle kinesin (*unc-104(e1265); oxIs91[*UNC-57-GFP; *lin-15+])*.

the distribution of the GFP-tagged synaptic vesicle protein synaptobrevin (also known as VAMP) in GABA neurons (Jorgensen et al., 1995). GFP fluorescence was punctate in wild-type animals, because the protein is associated with clusters of synaptic vesicles at neuromuscular junctions. In *unc-57(ok310)* mutants, GFP fluorescence was diffuse throughout both the dorsal and ventral cords as well as in commissural axons (Figure 4A). This phenotype is similar to the synaptobrevin mislocalization observed in other endocytosis mutants including the synaptojanin mutant *unc-26* (Harris et al., 2000; Nonet et al., 1999). To show that at a gross level nervous system development is not perturbed in *unc-57* mutants, we analyzed the structure of the GABA neurons (McIntire et al., 1997) in these animals and confirmed that axon outgrowth of these neurons occurred normally in the absence of endophilin protein (data not shown).

If there is a defect in synaptic vesicle endocytosis, then there should be a decrease in the number of synaptic vesicles at the synapse. We reconstructed a segment of the ventral nerve cord of wild-type and *unc-57* mutant animals using serial section electron microscopy. Wild-type animals were fixed in parallel and micrographs from the mutants and control animals were shuffled and scored blind. There was a severe depletion in the number of synaptic vesicles at the synapses of mutant animals as compared to wild-type animals (Figures 4B and 4C). In the wild-type, the mean number of synaptic vesicles per synapse was 200.7 $\pm$ 19.9 vesicles/synapse ($n = 28$ synapses). By contrast, in *unc-57(ok310)* animals the mean number of synaptic vesicles per synapse (70.5 $\pm$ 7.1 vesicles/synapse, $n = 38$ synapses) was reduced to 35% of wild-type levels ($p < 0.0001$), and in *unc-57(e406)* animals the mean number of synaptic vesicles per synapse (52.3 $\pm$ 5.8 vesicles/synapse, $n = 32$ synapses) was reduced to 26% of wild-type levels ($p < 0.0001$).

Endophilin mutant animals also had significantly fewer synaptic vesicles docked at the plasma membrane adjacent to active zones. There were 19.25 $\pm$ 1.95 docked vesicles per synapse in the wild-type. However, there were only 12% of the number of docked vesicles in *unc-57(ok310)* animals compared to the wild-type (2.32 $\pm$ 0.47 docked vesicles/synapse) and 21% of the number of docked vesicles in *unc-57(e406)* animals compared to the wild-type (4.09 $\pm$ 0.63 docked vesicles/synapse). When the number of docked vesicles is normalized to the total number of synaptic vesicles present at synapses, there is still a significant decrease in docked vesicles relative to the wild-type (wild-type = 10.58% $\pm$ 0.81% docked vesicles/synapse; *unc-57(ok310)* =

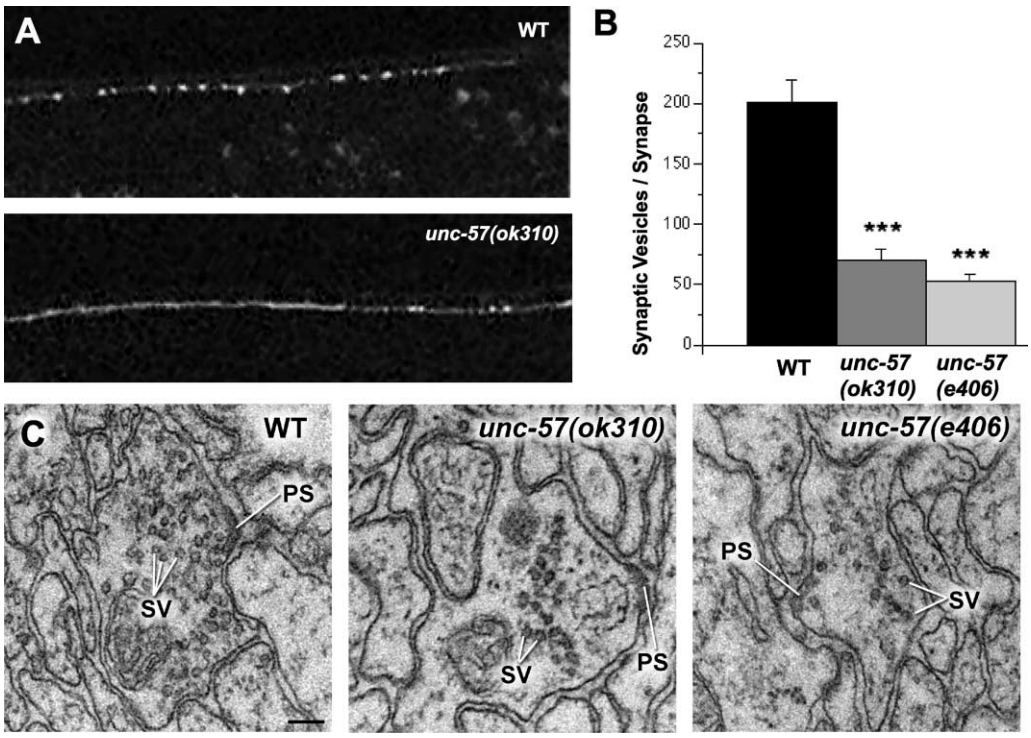

Figure 4. *unc-57* Mutants Have a Defect in Vesicle Recycling

(A) Synaptobrevin is mislocalized in *unc-57* animals. GABA neuromuscular junctions in the dorsal nerve cord are shown for an adult wild-type and *unc-57(ok310)* mutant animal. GFP-tagged synaptobrevin/VAMP (*nIs52)* is diffuse rather than punctate in *unc-57* animals compared to the wild-type consistent with a failure in vesicle protein retrieval. WT, the wild-type.

(B) Synaptic vesicles are depleted at synapses of *unc-57* mutants. *unc-57(ok310)* and *unc-57(e406)* mutants exhibit a reduction in the number of synaptic vesicles per neuromuscular junction (NMJ) compared to the wild-type (***$p < 0.0001$ for both genotypes). Synaptic vesicles were counted in reconstructed neuromuscular junctions (wild-type, 200.7 $\pm$ 19.9 SV/NMJ, n = 28 synapses; *unc-57(ok310),* 70.5 $\pm$ 7.1 SV/NMJ, n = 38 synapses; *unc-57(e406)*, 52.3 $\pm$ 5.8 SV/NMJ, n = 32 synapses).

(C) Sample electron micrographs of GABA neuromuscular junctions. Arrows point to the presynaptic specialization (PS) of the active zones; SV, synaptic vesicle; scale bar equals 100 nm.

4.7% $\pm$ 0.84% docked vesicles/synapse, $p < 0.0001$; *unc-57(e406)* = 7.65% $\pm$ 0.87% docked vesicles/synapse, $p = 0.013$). The decrease in docked synaptic vesicles detected in *unc-57* mutants is likely to be due to adhesion of vesicles in clusters away from the active zone (Figures 4C and 5C).

Endophilin Mutants Resemble Synaptojanin Mutants

The reduction in the number of synaptic vesicles in *unc-57(ok310)* (35% of wild-type) and *unc-57(e406)* (26% of wild-type) is very similar to the reduction observed in synaptojanin/*unc-26(s1710)* mutants (38%; Harris et al., 2000). We did a detailed ultrastructural characterization of synapses in endophilin mutants and found that they resemble synaptojanin mutant synapses in three ways (Table 1).

First, *unc-26* mutants accumulate endocytic intermediates, specifically clathrin-coated vesicles and endocytic pits. *unc-57* mutant animals also exhibited a significant increase in the number of clathrin-coated vesicles at synapses (Figure 5A). While these coated vesicles were never seen in the wild-type (n = 2 animals, 28 synapses), 2.7 $\pm$ 0.5 coated vesicles per synapse were observed in *unc-57(ok310)* animals (n = 2 animals, 38 synapses) and 1.7 $\pm$ 0.3 coated vesicles per synapse were observed in *unc-57(e406)* animals (n = 2 animals, 32 synapses). Other endocytic intermediates seen less frequently were pits (typically uncoated) adjacent to active zones (Figure 5B). While only one endocytic pit was observed in one synapse of the wild-type (0.035 $\pm$ 0.035 pits per synapse), 65.8% of the synapses in *unc-57(ok310)* (1.24 $\pm$ 0.19 pits per synapse) and 34.4% of the synapses in *unc-57(e406)* (0.41 $\pm$ 0.11 pits per synapse) had endocytic pits (both values are statistically significant: $p < 0.0001$ for *unc-57(ok310)*; $p = 0.034$ for *unc-57(e406)*).

Second, *unc-26* mutants exhibit an abnormal distribution of synaptic vesicles away from the active zone, and these vesicles are arranged on fibers. The distribution of synaptic vesicles was also altered in endophilin mutants. Vesicles were found distal from the active zone and were organized in long arrays of vesicles connected through filamentous networks, giving the appearance of a "string-of-pearls" phenotype (Figure 5C). This phenotype was observed in only 1 of 28 (3.6%) synapses in the wild-type, but was seen in 31 of 38 synapses (81.6%) in *unc-57(ok310)* animals and 20 of 32 synapses (62.5%) in *unc-57(e406)* animals.

Third, *unc-26* mutants exhibit an accumulation of cisternae. The absence of endophilin also resulted in an

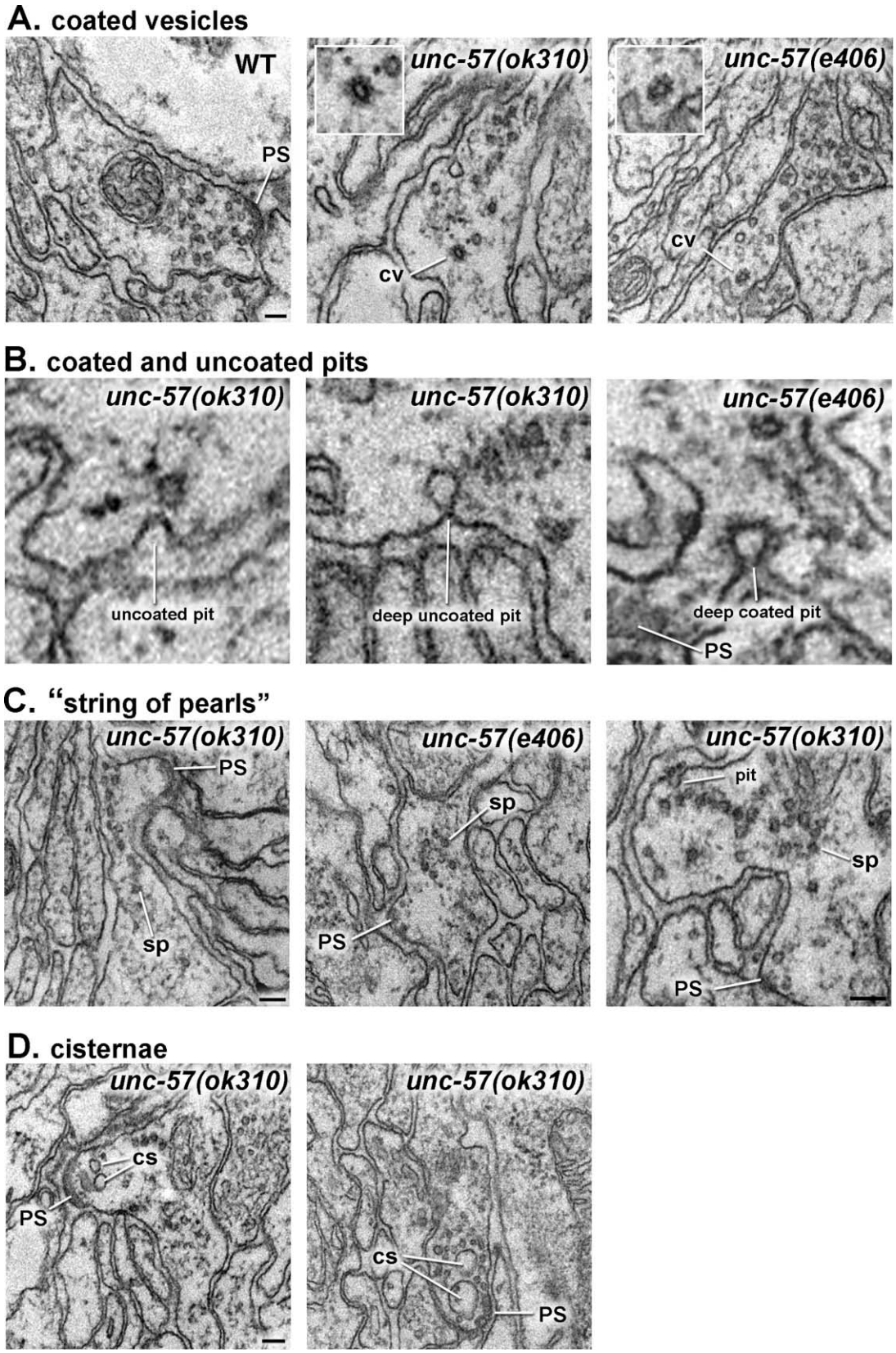

Figure 5. Endophilin Mutants Exhibit the Same Ultrastructural Defects as Synaptojanin Mutants

(A) Coated vesicles. *unc-57(ok310)* and *unc-57(e406)* animals show an accumulation in clathrin-coated vesicles at synapses. A neuromuscular junction is shown for the indicated genotypes. Wild-type animals had no observable clathrin-coated vesicles, compared to a total of 107 and

Table 1. Summary of Electron Microscopy Results

	Wild-Type	*unc-57(ok310)*	*unc-57(e406)*
Total number of synapses scored	28	38	32
Synaptic vesicles per synapse	200.7 ± 19.9	70.5 ± 7.1	52.3 ± 5.8
Docked SVs per synapse	19.25 ± 1.95	2.32 ± 0.47	4.09 ± 0.63
Mean endocytic pits	0.035 ± 0.035	1.24 ± 0.19	0.41 ± 0.11
Clathrin-coated vesicles per synapse	0	2.7 ± 0.5	1.7 ± 0.3
% synapses with string-of-pearls	4% (1/38)	82% (31/38)	63% (20/32)
Cisternae per synapse	0.64 ± 0.07	1.39 ± 0.10	0.89 ± 0.07
Number of synapses/10 μM	16	21	19

accumulation of cisternae at synapses, typically near active zones (Figure 5D). Specifically, *unc-57* animals exhibited a 2.2-fold (*ok310*) and a 1.4-fold (*e406*) increase in these structures when compared to the wild-type. Wild-type animals had a mean of 0.64 ± 0.07 cisternae per section, compared to 1.39 ± 0.10 cisternae per section for *unc-57(ok310)* ($p < 0.0001$) and 0.89 ± 0.07 cisternae per section for *unc-57(e406)* ($p = 0.014$). Thus, the same ultrastructural defects observed in synaptojanin mutants are also observed in endophilin mutants.

Endophilin Mutants Exhibit Defects in Neurotransmission

The similarity of the phenotypes observed for endophilin (*unc-57*) and synaptojanin (*unc-26*) mutants suggest that these proteins function in the same pathway. The genetic test to determine whether two proteins function in a pathway is to determine the phenotype of the double mutant. If two proteins act in the same pathway, then the double mutant should be no more severe than the single mutants. Such analyses must be performed on a quantitative phenotype to be meaningful. A quantitative and sensitive assay for a defect in synaptic transmission is voltage-clamp recording from the body muscle of the adult nematode. Three electrophysiological assays from the body muscles demonstrated that synaptic transmission defects are identical in *unc-57* mutants and in *unc-26* mutants. More importantly, *unc-57 unc-26* double mutants exhibited the same defect as the single mutants.

First, we recorded endogenous synaptic currents without stimulation. One can resolve the fusion of single synaptic vesicles in this assay (Figure 6A). The size of miniature postsynaptic currents (minis) caused by the release of one or a few vesicles were the same in all genotypes, suggesting that the postsynaptic receptor field in these strains is normal (Figure 6B). However, endogenous rates of synaptic vesicle fusions were reduced to ~15%, compared to the wild-type frequency in both *unc-57(e406)* and *unc-57(ok310)* mutant animals (Figure 6C). The frequency of endogenous events for wild-type animals was 77 ± 3.9 fusions per second ($n = 40$), whereas for *unc-57(e406)* and *unc-57(ok310)* the frequency was 11 ± 1.4 and 13 ± 1.94 fusions per second, respectively ($n = 8$ and $n = 16$). Similarly, the endogenous frequency of synaptic vesicle fusions in *unc-26(s1710)* was reduced to 12 ± 1.9 fusions per second ($n = 12$) compared to the wild-type, which was not different from either of the *unc-57* mutants. Mini frequencies in *unc-57(e406) unc-26(s1710)* and *unc-57(ok310) unc-26(s1710)* double mutants were reduced to 17 ± 1.9 ($n = 12$) and 16 ± 1.7 ($n = 19$) fusions per second, respectively. In neither case were the double mutants more severe than the single mutants.

Second, we recorded evoked currents caused by a single stimulation of the nerve cord. This assay measures the number of synaptic vesicles released upon calcium influx. Evoked current amplitudes in *unc-57(e406)* and *unc-57(ok310)* were reduced to ~60% (58% and 57%, respectively) of the evoked currents in the wild-type (Figure 6D). Evoked responses in the wild-type were 2428 ± 169 pA ($n = 28$), whereas evoked responses were significantly decreased in the *unc-57* mutants (1404 ± 156 pA, $n = 10$ for *unc-57(e406)*; 1378 ± 100 pA, $n = 14$ for *unc-57(ok310)*, $p = .0001$). Similar evoked responses were observed in *unc-26(s1710)* (1126 ± 137 pA, $n = 13$) and in the *unc-57(e406) unc-26(s1710)* (1085 ± 216 pA, $n = 9$) and *unc-57(ok310) unc-26(s1710)* double mutants (1155 ± 153 pA, $n = 6$). None of the single or double mutants were significantly different from each other ($p > 0.24$), but all were significantly reduced compared to the wild-type.

Third, we measured the decline in evoked response caused by multiple stimulations. The fatigue rate measures the size of, or access to, the reserve pool of vesicles. *unc-57* mutants fatigued more rapidly than the wild-type (Figure 6E). After 10 stimulations, evoked current amplitudes in the wild-type were 52% ± 4.1% (n =

53 clathrin-coated vesicles observed in mutant animals (*unc-57(ok310)* and *unc-57(e406)* animals, respectively). Scale bar equals 100 nm. Inset is enlargement of the coated vesicle observed in the micrograph. PS, presynaptic specialization; cv, coated vesicle; sp, string-of-pearls, indicates vesicles attached to a cytoskeletal lamina; cs, cisterna.

(B) Pits. *unc-57(ok310)* and *unc-57(e406)* animals show an accumulation of both uncoated and coated pits in the plasma membrane near active zones. Shown are uncoated pits and coated and uncoated deeply invaginated pits. Arrow, active zone.

(C) String-of-pearls. *unc-57(ok310)* and *unc-57(e406)* mutants exhibit a shift in the distribution of vesicles away from the electron-dense region of the synapse. These vesicles are often in a row and are attached to a filamentous network. This string-of-pearls phenotype was observed in 81.6% of synapses in *unc-57(ok310)* animals and 62.5% of synapses in *unc-57(e406)* animals, compared to 3.6% of synapses in wild-type animals. Arrow, active zone; scale bar equals 100 nm.

(D) Cisternae. *unc-57* animals show an accumulation of cisternae at synapses. Shown are representative micrographs depicting endosomal-like membranous structures located near active zones in *unc-57(ok310)* and *unc-57(e406)* animals. Arrow, active zone; scale bar equals 100 nm.

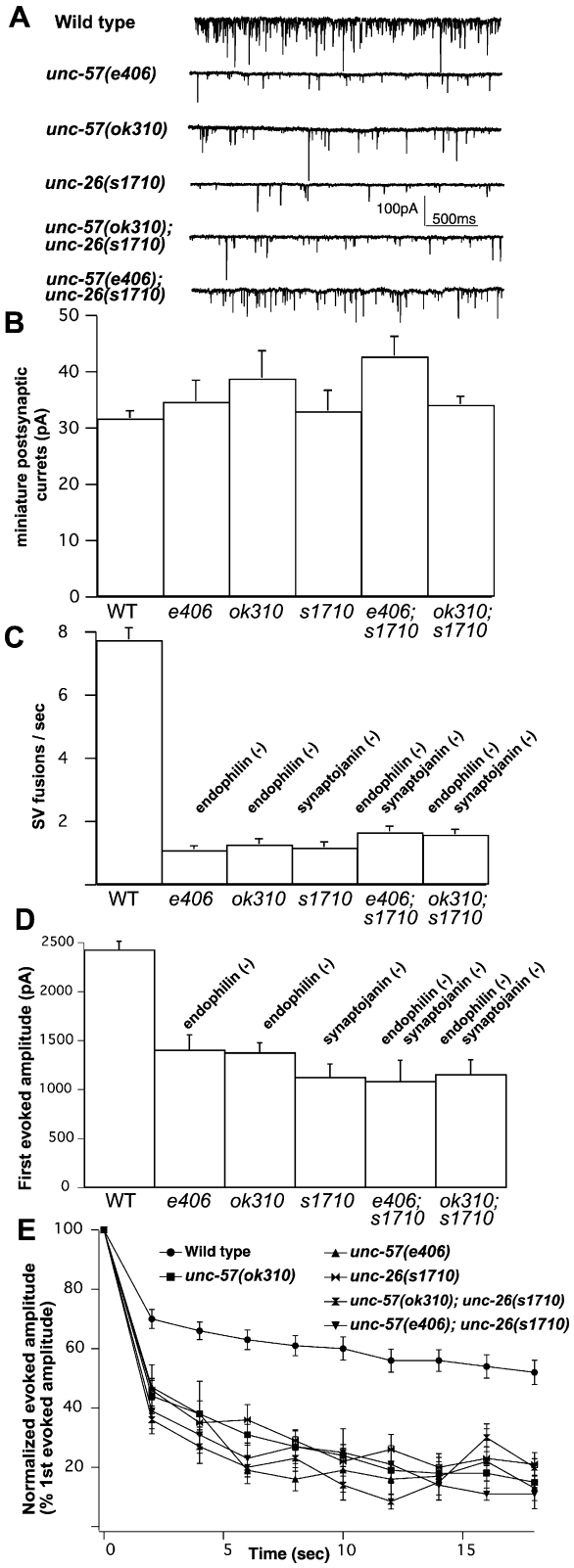

Figure 6. Endophilin Mutants Have the Same Electrophysiological Phenotype as Synaptojanin Mutants

(A) Endogenous minis. Miniature postsynaptic currents (minis) were measured in whole-cell voltage-clamp recordings of body muscles of adult hermaphrodites. Miniature currents are caused by neurotransmitter released from one or a few vesicles. Sample traces are shown.

(B) Mini amplitudes. The current amplitudes of the minis are unaltered in *unc-57*, *unc-26*, and *unc-57; unc-26* double mutants, indicating that the postsynaptic field is intact.

(C) Mini frequencies. The average frequencies of vesicle fusions compared to wild-type animals were reduced by 89% in *unc-57(e406)*, 87.5% in *unc-57(ok310)*, 90% in *unc-26(s1710)* double mutants, and 87.5% in *unc-57(ok310);unc-26(s1710)* double mutants.

(D) Evoked currents. The ventral nerve cord was stimulated by a single 2 ms depolarization, and the maximum evoked current amplitudes were measured in body muscles. Maximum currents were reduced to a similar extent in *unc-57, unc-26*, and *unc-57; unc-26* double mutants.

(E) Fatigue. Trains of ten depolarizing stimuli were delivered to the ventral nerve cord at 0.5 Hz and evoked currents measured in body muscles. Currents at each stimulus were calculated as a percentage of the first current for each genotype. Repeated stimuli caused a 48% depression of the wild-type evoked current amplitude, whereas *unc-57* alleles *(e406)* and *(ok310)* were reduced 89% and 85%, respectively; *unc-26(s1710)* was reduced 79%, the double mutant *unc-57(e406); unc-26(s1710)* was reduced 89%, and *unc-57(ok310); unc-26(s1710)* was reduced 80%. All muscle recordings were conducted at a holding potential of −60 mV in the whole-cell mode in extracellular Ringer's containing 5 mM calcium, and data are presented as mean and SEM.

26) compared to the first stimulation, whereas the evoked currents were 11% ± 2.2% (n = 9) in *unc-57(e406)* and 15% ± 2.3% (n = 13) in *unc-57(ok310)*. These data suggest that *unc-57* mutants have a pool of synaptic vesicles that can be released upon stimulation but that the pool is depleted more rapidly than in wild-type worms. More importantly, synaptojanin mutants are not exacerbated by the addition of mutations in endophilin. *unc-26(s1710)* trains were reduced to 21% ± 5% (n = 11), and the *unc-57(e406) unc-26(s1710)* and *unc-26(s1710) unc-57(ok310)* double mutants were reduced to 11% ± 2.2% (n = 9, $p > .05$) and 20% ± 2.9% (n = 3, $p > 0.49$) of the first stimulation, respectively. Therefore, in all three assays, *unc-57* mutants, *unc-26* mutants, and *unc-57 unc-26* double mutants had equivalent neurotransmission defects.

Overexpression of Synaptojanin Does Not Rescue Endophilin Mutants

The double mutant data demonstrate that endophilin acts in the same pathway as synaptojanin, but it does not distinguish whether endophilin acts on synaptojanin or whether synaptojanin acts on endophilin. Often a defect in a molecular pathway can be corrected by overexpressing or constitutively activating a downstream component of the pathway. We tested whether overexpression of synaptojanin could rescue endophilin mutants and whether overexpression of endophilin could rescue synaptojanin mutants. Minigenes with GFP tags were constructed for both synaptojanin and endophilin. High-copy transgenic arrays were generated by microinjection and then integrated into chromosomal DNA to insure stable inheritance. The tagged protein constructs for UNC-26 and UNC-57 rescued *unc-26* and *unc*-57 mutants, respectively; thus, the proteins generated by these transgenes are expressed and functional (Figure 7).

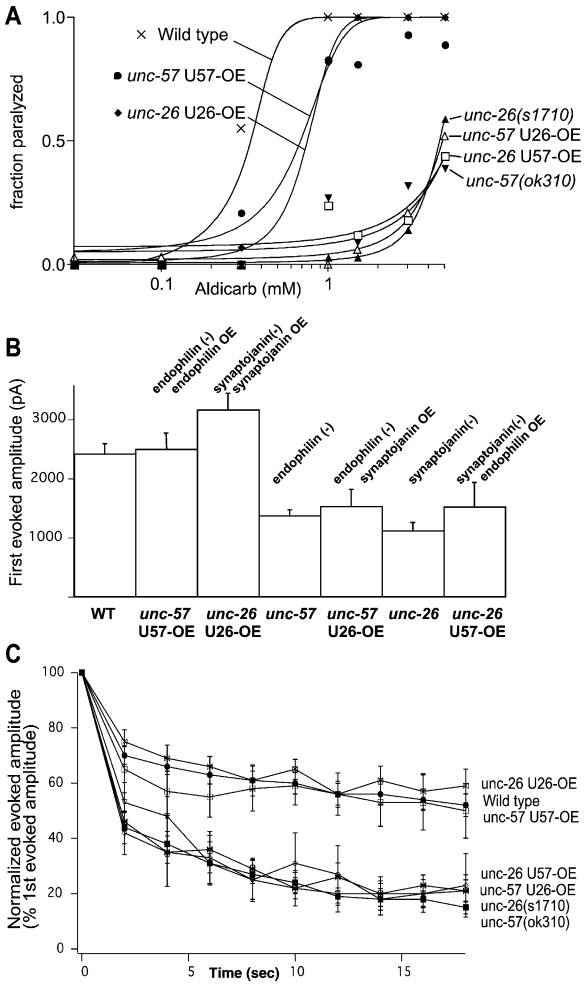

Figure 7. Overexpression of Synaptojanin or Endophilin

(A) Aldicarb resistance. Adult hermaphrodites were placed on agar containing the indicated concentrations of Aldicarb, which is an inhibitor of acetylcholineesterase (Yook et al., 2001). In the presence of this drug, acetylcholine is not degraded and chronically stimulates muscle contraction. Treated animals become paralyzed. Mutants lacking endophilin or synaptojanin were both strongly resistant to the drug. A transgene expressing synaptojanin (*oxIs92* "U26-OE") rescued Aldicarb sensitivity of *unc-26(s1710)*. However, overexpression of synaptojanin did not rescue *unc-57(ok310)*. A transgene expressing endophilin (*oxIs91*, "U57-OE") rescued Aldicarb sensitivity of *unc-57(ok310)*. However, overexpression of endophilin did not rescue *unc-26(s1710)*.

(B) Evoked currents. The maximum evoked current amplitudes were measured from whole-cell voltage-clamped muscles of adult hermaphrodites. Evoked responses of *unc-57(ok310)* mutants were rescued by the transgene expressing endophilin (*oxIs91*, "U57-OE"). Similarly, the maximum evoked current amplitudes of *unc-26(s1710)* mutants were rescued by the transgene expressing synaptojanin (*oxIs92*, "U26-OE"). However, overexpression of synaptojanin did not rescue *unc-57(ok310)* evoked currents, nor did overexpression of endophilin rescue *unc-26(s1710)* evoked currents.

(C) Fatigue. Trains of ten depolarizing stimuli were delivered at 0.5 Hz and evoked currents measured in voltage-clamped body muscles. Currents at each stimulus were calculated as a percentage of the first evoked response for each genotype and plotted on the graph. Sustained evoked neurotransmitter release was restored to wild-type levels in *unc-57(ok310)* mutants expressing endophilin (U57-OE) and in *unc-26(s1710)* mutants expressing synaptojanin (U26-OE). However, overexpressing synaptojanin in endophilin mutants (*unc-57(ok310); oxIs92)* or overexpressing endophilin in synaptojanin mutants (*unc-26(s1710); oxIs91)* failed to prevent rapid fatigue.

The synaptojanin multicopy array (U26-OE) was crossed into an endophilin mutant background (*unc-57(ok310))*. This strain was wild-type at the *unc-26* locus; thus, synaptojanin expression was the sum of protein expressed from the endogenous locus and the transgene. The strain was tested for rescue using three assays: Aldicarb sensitivity, evoked responses, and fatigue. Aldicarb is an acetylcholinesterase inhibitor; treated animals accumulate acetylcholine and become paralyzed. Aldicarb sensitivity is an assay in which both increases and decreases in neurotransmitter release can be detected. We observed that endophilin mutants were strongly resistant to Aldicarb and that overexpression of synaptojanin in this strain did not alter the resistance of the *unc-57* mutants (Figure 7A). Evoked responses from endophilin mutants were also unaffected by overexpressing synaptojanin (Figure 7B). Specifically, the average evoked amplitude in *unc-57(ok310)* overexpressing synaptojanin was 1538 $\pm$ 285 pA ($n = 7$), which was not significantly different from *unc-57(ok310)* alone (1378 $\pm$ 100, $n = 14$; $p > 0.5$). Finally, the increased fatigue observed in endophilin mutants was similarly unaffected by synaptojanin overexpression (Figure 7C). Fatigue after 10 stimulations in *unc-57(ok310)* overexpressing synaptojanin was 21% $\pm$ 5.9% ($n = 7$) compared to 15% $\pm$ 2.3% ($n = 13$, $p > 0.26$).

The endophilin multicopy array (U57-OE) was crossed into a synaptojanin mutant background (*unc-26(s1710))*. Synaptojanin mutants were equally resistant to Aldicarb as endophilin mutants. Overexpression of endophilin in *unc-26* mutants did not alter the resistance of strain (Figure 7A). Evoked responses from synaptojanin mutants were also unaffected by overexpressing endophilin in this mutant background (Figure 7B); average evoked amplitudes for *unc-26(s1710)* were 1126 $\pm$ 137 pA ($n = 13$), compared to amplitudes of 1531 $\pm$ 411 pA ($n = 5$) for *unc-26(s1710)* overexpressing endophilin ($p > 0.24$). Finally, the increased fatigue observed in synaptojanin mutants (23% $\pm$ 11.5% first response, $n = 4$) was similarly unaffected by endophilin overexpression, compared to *unc-26(s1710)* alone (21% $\pm$ 3.7%, $n = 13$, $p > 0.8$) (Figure 7C).

If synaptojanin acts downstream of endophilin, these data suggest that synaptojanin requires binding to endophilin either for membrane localization or for the activation of the phosphatase activity of synaptojanin. Alternatively, endophilin acts downstream of synaptojanin and the LPAAT activity of endophilin requires synaptojanin binding for activation.

Synaptojanin Expression and Localization Requires Endophilin

The double mutant data and the overexpression data demonstrate that endophilin acts in the same pathway as synaptojanin, but they do not distinguish whether endophilin acts on synaptojanin or whether synaptojanin acts on endophilin. To determine whether one of these proteins serves a docking role for the other, we determined endophilin and synaptojanin localization in mutant animals. The tagged protein constructs for UNC-26 and UNC-57 rescued *unc-26* and *unc-57* mutants, respectively; thus, at least some of each of these proteins must be localized properly.

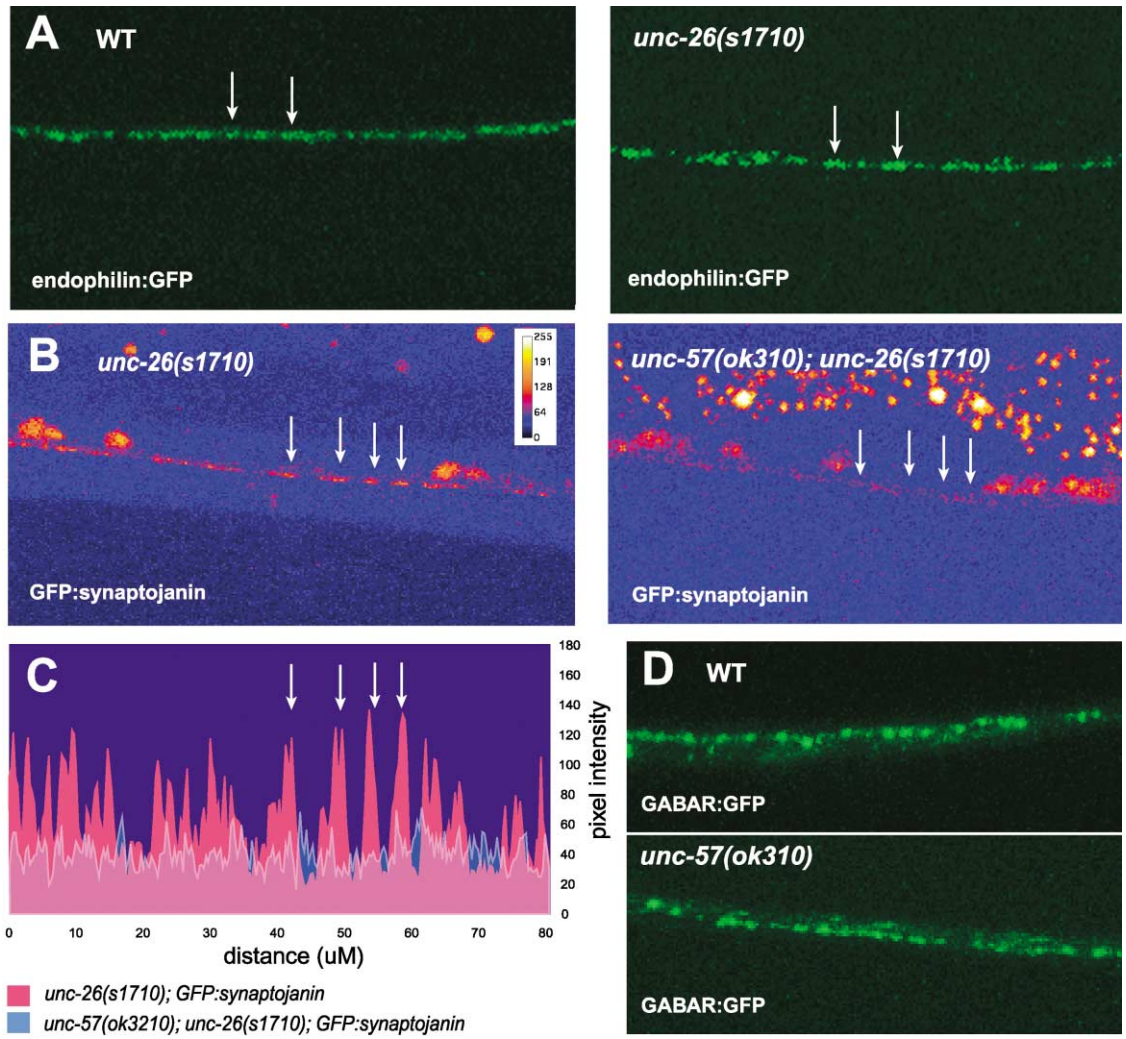

Figure 8. Localization of Tagged Endophilin and Synaptojanin in Mutants

(A) Endophilin distribution. GFP-tagged endophilin was localized to puncta likely to be neuromuscular junctions in the dorsal nerve cord of wild-type animals (genotype *lin-15(n765) oxIs91 X*). GFP-tagged endophilin was also localized to puncta in the dorsal nerve cord of *unc-26* mutants (genotype *unc-26(s1710); lin-15(n765) oxIs91*). WT, the wild-type.

(B) Synaptojanin distribution. GFP-tagged synaptojanin was localized to puncta at neuromuscular junctions (white arrows) in the ventral nerve cord of *unc-26* animals (genotype *oxIs92 II; unc-26(s1710) IV*) but was reduced and diffuse in *unc-57* animals (genotype *unc-57(ok310) I; oxIs92 II; unc-26(s1710) IV*). White arrows indicate alignment of the left panel arrows over the right panel as shown merged in (C).

(C) Fluorescence intensity. Graphic representation of the fluorescence intensity of the ventral cords shown in (B). *unc-26(s1710)* is shown in hot pink, *unc-57(ok310); unc-26(s1710)* is shown in blue, and the overlap between the two graphs is shown in light pink. The arrows in (B) and (C) point to the same four puncta present in the *unc-26(s1710)* cord. There were no puncta visible in the *unc-57(ok310); oxIs92; unc-26(s1710)* animals.

(D) GABA receptor distribution. The GABA receptor, encoded by the *unc-49* gene, is clustered on muscles at neuromuscular junctions in the wild-type (genotype *oxIs22[UNC-49::GFP]*). The GABA receptor is normally localized in endophilin mutants (genotype *unc-57(ok310); oxIs22[UNC-49::GFP]*). These data indicate that the absence of synaptojanin puncta in endophilin mutants is not caused by a failure in synapse formation.

GFP-tagged endophilin was localized correctly to synapses in *unc-26(s1710)* mutant animals and was in fact brighter than in wild-type animals (Figure 8A). By contrast, synaptojanin-GFP appeared to be reduced in levels and was diffuse in *unc-57(ok310)* mutants (Figure 8B), compared to the wild-type. Quantitative fluorescence microscopy was performed to verify these observations. Average synaptojanin-GFP fluorescence intensity was determined for the cell bodies and ventral cord in endophilin/*unc-57* mutant and control worms. Fluorescence was reduced in *unc-57(ok310)* mutants by 16% in the cell bodies (average intensity on scale of 0 to 255: 98.5 in the control, 82.6 in *unc-57(ok310)*, $p = 0.0006$) and 25% in the ventral cord (average intensity is 70.5 in the control and 53.0 in *unc-57(ok310)*, $p = 0.001$). The loss of synaptojanin in axons was caused by a specific loss of accumulation at synapses (Figure 8B). Line graphs were made of the ventral cord of control and *unc-57(ok310)* worms. Peaks of fluorescence, corresponding to punctate localization of synaptojanin-

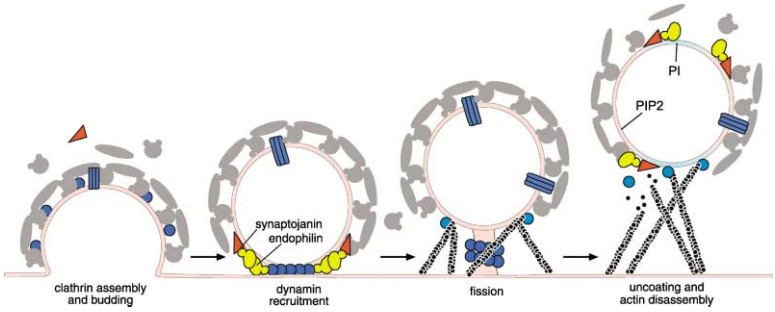

Figure 9. Model for Endophilin Function

PIP_2 recruits clathrin adaptor proteins to membrane domains targeted for recycling (Gaidarov and Keen, 1999; Hao et al., 1997), which promotes vesicle budding. Endophilin binds to lipids and proteins and recruits synaptojanin, thereby bringing synaptojanin to its lipid substrate PIP_2. PIP_2 degradation by synaptojanin or a lipid-shaping function of endophilin may be required for a step during fission, because in synaptojanin and endophilin mutants, uncleaved vesicles accumulate. Actin polymerization, regulated by PIP_2, drives the budded vesicle away from the plasma membrane and thus aids in the separation of the vesicle from the plasma membrane. Dephosphorylation of $PI(4,5)P_2$ to PI by synaptojanin causes adaptor proteins and actin polymerization machinery to dissociate from the vesicle.

GFP, were observed in control worms. *unc-57(ok310)* mutant worms did not exhibit peaks of fluorescence, but levels were constant along the length of the cord at the same levels as intersynaptic regions of the control (Figure 8C). The loss of synaptojanin at synapses in *unc-57* is not caused by a defect in synapse formation. Normal postsynaptic clusters of GABA receptors (Bamber et al., 1999) were observed at neuromuscular junctions along the ventral nerve cord of *unc-57* mutants (Figure 8D). These data indicate that in the absence of endophilin protein, synaptojanin is mislocalized, while in the absence of synaptojanin protein, endophilin is correctly localized. Thus, endophilin localizes synaptojanin to synapses.

Discussion

Endophilin Is Required for Synaptic Vesicle Recycling

Our characterization of *unc-57* mutants indicates that endophilin is required for synaptic vesicle recycling via clathrin-mediated endocytosis in *C. elegans* neurons. First, the synaptic vesicle protein synaptobrevin/VAMP is mislocalized in endophilin mutants, consistent with a failure in protein retrieval from the plasma membrane. Second, there is a severe depletion of synaptic vesicles at the neuromuscular junction in *unc-57* mutants compared to the wild-type. Third, there is a physiological depletion of synaptic vesicles; the frequency of synaptic vesicle fusions is decreased by 86% in *unc-57* mutants. This value corresponds well to the 86% depletion of vesicles docked at the plasma membrane in these animals.

Synaptojanin Function Requires Endophilin

A comparison of *unc-57* and *unc-26* mutants indicates that endophilin and synaptojanin proteins are required for the same process. First, endophilin (*unc-57*) and synaptojanin (*unc-26*) single mutants have identical phenotypes as analyzed by drug studies and by electrophysiology. Importantly, they exhibit rapid synaptic fatigue, which is consistent with a defect in synaptic vesicle endocytosis. Second, endophilin and synaptojanin mutants both exhibit unusual ultrastructural phenotypes. Specifically, *unc-57* and *unc-26* mutant synapses are depleted of synaptic vesicles, accumulate coated vesicles, and exhibit strings of synaptic vesicles attached to filaments away from the active zone. Third, *unc-57 unc-26* double mutants have the same quantitative electrophysiological phenotype as either the *unc-26* or *unc-57* single mutants, suggesting that these proteins function in the same pathway. Fourth, synaptojanin is not localized to synapses in endophilin mutants, while endophilin appears to be correctly localized in synaptojanin mutants. This leads us to propose a model in which endophilin is an adaptor protein that recruits synaptojanin to its substrate $PI(4,5)P_2$ (Figure 9).

Endophilin A has been shown to bind dynamin (de Heuvel et al., 1997; Micheva et al., 1997b; Modregger et al., 2003; Ringstad et al., 1997). Unlike endophilin A mutants, dynamin mutants are required for viability in *C. elegans* (A.M.v.d.B., data not shown). Our data indicate that endophilin A and synaptojanin functions are overlapping. How might dynamin fit into endophilin function then? There are two possibilities. First, the dynamin-endophilin interaction may be required for the functioning of the synaptojanin-endophilin complex during endocytosis. Second, dynamin might not interact with endophilin A in vivo, but rather dynamin interacts with endophilin B, which binds dynamin but not synaptojanin (Modregger et al., 2003) or the related SH3 domain-containing protein amphiphysin (David et al., 1996).

The data described here demonstrate that endophilin and synaptojanin function as a complex. In the simplest model, endophilin localizes synaptojanin to particular patches of membrane from which PIP_2 must be degraded. However, it is also possible that endophilin has functions that require synaptojanin. For example, endophilin might require synatojanin binding to activate membrane remodeling via its lysophosphatidic acid acyl transferase (LPAAT) activity (Schmidt et al., 1999). Tests of this model will require biochemical characterization of the LPAAT activity in the absence or presence of synaptojanin.

Experimental Procedures

C. elegans Strains

The *ok310* deletion was obtained from the *C. elegans* gene knockout project at OMRF, which is part of the International *C. elegans* Gene-Knockout Consortium (http://www.mutantfactory.ouhsc.edu) and outcrossed twice before being used for experiments (EG2710). EG3027: *unc-26(s1710)* outcrossed once. EG3028: *unc-57(e406)* outcrossed twice. The strains used for injection are: EG2813, *unc-57(ok310); lin-15 (n765ts)*; and EG2935, *unc-26(s1710) ; lin-15*

(n765ts). GFP-expressing strains are as follows: EG3034, *oxEx481-[Punc-57:GFP]; lin-15(n765ts)*; EG3031, *oxIs91[UNC-57:GFP, lin-15+];lin-15(n765ts)*; EG3032, *unc-26(s1710); oxIs91[UNC-57:GFP, lin-15+]*; EG3036, *unc-104(e1265); oxIs91[UNC-57:GFP, lin-15+]*; EG3048, *oxIs92[GFP:UNC-26, lin-15+]; unc-26(s1710)*; EG3055, *unc-57(ok310); oxIs92[GFP:UNC-26, lin-15+]; unc-26(s1710)*. The strains used in the overexpression study are: EG3048, *oxIs92[GFP: UNC-26, lin-15+]; unc-26(s1710)*; EG3032, *unc-26(s1710); oxIs91-[UNC-57:GFP, lin-15+]*; EG3044, *unc-57(ok310);oxIs91[UNC-57:GFP, lin-15+]; lin-15(n765ts)*; EG3035, *unc-57(ok310); oxIs92-[GFP:UNC-26, lin-15+]*. The double mutant strains are: EG3038, *unc-57(ok310); unc-26(s1710)* and *unc-57(e406); unc-26(s1710)*. The synaptobrevin (VAMP):GFP strain used is EG2827, *unc-57(ok310); nIs52*. The GABA receptor (*unc-49*):GFP strain is EG1653, *oxIs22-[unc-49:GFP, lin-15+]*.

cDNA Identification and Sequence

cDNAs, yk1305d and yk1027b, corresponding to the T04D1.3 open reading frame were contained in the collection of cDNAs isolated by Yuji Kohara (http://nematode.lab.nig.ac.jp/dbest/keysrch.html).

GFP Expression Constructs

pKS30: u57GFPntx Transcriptional GFP Construct

A 4.5 kb promoter fragment upstream of the T20D1.3 ORF was amplified from the cosmid T04D1 using primers u57ntx1: TAATA GATCCTTCCGATGAATCGG and u57ntx2: GGCATGCTTTTCTGAA AATTTTGAGTTTTAGATTCGG. The resulting 4.5 kb fragment was TA cloned into the pCR2.1 vector (Invitrogen). A SmaI to ApaI fragment containing GFP and the *unc-54* termination sequence from the Fire vector, pPD95.67, was cloned into the EcoRV and ApaI sites of pCR2.1. pKS30 was injected into *lin-15(n765ts)* worms at a concentration of 25 ng/μl along with EK L15 (60 ng/μl) to generate *oxEx481*.

pDR1: unc-57 Rescue Construct

2 kb of upstream endophilin promoter sequence was amplified by PCR from genomic DNA using primers of sequence GCGAAGCTTT CCAATTTTTTTCAAATATCCGC and GTCGATACGTTTCTGCAG CATCG and was subcloned into the Fire vector pPD95.81 using HindIII and PstI. The 3′ end of the endophilin gene was PCR amplified from N2 genomic DNA using primers of sequence CGCGGATCCT CAAAATTTTCAGAAAAATGTCGTTG and CGCACCGGTTACGGTAC CTTAAGAGGCACTAGAACCTGTAC, which contains an AgeI restriction site. The endophilin rescue construct was made by subcloning the 3′ end of the endophilin gene into the endophilin promoter-containing construct using PstI and AgeI. pDR1 was injected into *unc-57(ok310); lin-15(7765ts)* at a concentration of 20 ng/μl along with the co-injection marker P*unc-122*:GFP (60 ng/μl) (gift of P. Sengupta) to generate *oxEx422* and *oxEx423*.

pKS31: U57GFPctI Translational Construct

This construct was made essentially as described for pDR1 except that the 3′ end of the endophilin gene was cloned into the endophilin promoter construct using PstI and KpnI. pKS31 was injected into *unc-57(ok310); lin-15(n765ts)* worms at a concentration of 0.75 ng/μl along with EK L15 (50 ng/μl) (Clark et al., 1994) and 1 kb ladder (50 ng/μl) to generate *oxEx462*. EG2941 containing *oxEx462* was irradiated with 4000 Rads of X-ray to obtain an integrated array *oxIs91[*UNC-57-GFP*; lin-15(+)]*.

pKS32: u26GFPntI Translational Construct

A NotI site was created in pPD95.67 (pPD95.67NotI) by PCR amplifying GFP using GFP 5′: GAAGAAGCGTAAGGTACCGGTAG and GFPNot: GAATTCGCGGCCGCTTTGTATAGTTCATCCATGCCATG. The *unc-26* cDNA, yk453b7 from Yuji Kohara, was used as template in order to create NotI sites on either side of the *unc-26* sequence, u26NotI: GCGGCCGCTATGTCAGTTCGAGGGATTCGG and u26Not2: GCGGCCGCTCTACATATTTTTTGGTCTAGGTGG, and was cloned into the NotI site of the vector pPD95.67NotI. The UNC-26:GFP fusion is driven by the neuron-specific *rab-3* promoter (Nonet et al., 1997) using a PstI fragment (Marc Hammarlund, personal communication). pKS32 was injected into *unc-26(s1710); lin-15(n765ts)* worms at a concentration of 7 ng/μl along with EK L15 (50 ng/μl) and 1 kb ladder (45 ng/μl) to generate *oxEx475*. The strain EG3000 containing *oxEx475* was irradiated with 4000 Rads of X-ray to obtain an integrated array *oxIs92[*GFP-UNC-26; *lin-15(+)]*.

Electrophysiology

Methods were as previously described. Briefly, animals were immobilized and dissected as to expose the ventral medial body wall muscle. Whole-cell voltage clamp was performed (holding potential, −60 mV) at room temperature using an EPC-9 patch-clamp amplifier (HEKA, Germany) and digitized at 2.9 kHz via an ITC-16 interface (Instrutech, NY). Data were acquired using HEKA Pulse software. A fire-polished electrode positioned close to the ventral nerve cord was used to stimulate evoked neurotransmission using a 2 ms depolarization. The bath solution contained 140 mM NaCl, 5 mM KCl, 6 mM $CaCl_2$, 5 mM $MgCl_2$, 11 mM glucose, and 5 mM HEPES (pH 7.2), 330 mOsm. The pipette solution contained 120 mM KCl, 20 mM KOH, 4 mM $MgCl_2$, 5 mM N-tris [Hydroxymethyl] methyl-2-aminoethane-sulfonic acid, 0.25 mM $CaCl_2$, 4 mM NaATP, 36 mM sucrose, and 5 mM EGTA (pH 7.2), 315 mOsm. Data were analyzed and graphed using Pulsefit (HEKA), Mini Analysis (Jaejin), and Igor Pro (Wavemetrics, OR).

Electron Microscopy

Wild-type (N2), *unc-57(ok310),* and *unc-57(e406)* adult nematodes were prepared in parallel for transmission electron microscopy as previously described (Jorgensen et al., 1995). Briefly, animals were immersed in ice-cold fixative (0.7% gluteraldehyde, 0.7% osmium tetroxide in 10 mM HEPES) for 1 hr. Nematode heads and tails were removed by cutting in fixative, and the bodies fixed again in 2% osmium tetroxide in 10 mM HEPES for 3 hr. Fixed specimens were washed in water, stained in 1% uranyl acetate, dehydrated through an ethanol series, washed in propylene oxide, and embedded in epoxy resin. Ribbons of ultrathin (∼40 nm) serial sections were collected. Images were obtained on a Hitachi H-7100 electron microscope using a Gatan slow scan digital camera by W.S.D. Mutant and control sections were shuffled and then scored blind by a second individual (D.S.M.) who was unaware of the genotypes. >200 ultrathin contiguous sections were cut and the ventral nerve cord reconstructed from two animals representing each genotype (total of 1297 sections from 6 different animals). Image analysis was performed using NIH Image software.

Quantitation

All quantitation was obtained from cholinergic neurons VA and VB and the γ-aminobutyric (GABA) neuron VD (White et al., 1976). A synapse was defined as the serial sections containing a presynaptic density as well as two sections on either side of that density. Docked vesicles were defined as those vesicles that were contacting the plasma membrane adjacent to the presynaptic density and juxtaposed to muscle. Vesicles defined as "close" were those that were within one vesicle diameter (35 nm) from the plasma membrane.

Quantitative Fluorescent Microscopy

Images were collected using a 40× objective on a Biorad Radiance 2000 confocal microscope. Animals were immobilized with 2% phenoxypropanol and rotated such that their ventral cords were facing up. The same region of the ventral cord, anterior of the vulva, was imaged in each worm and all images were obtained using the same settings, on the same day, using a laser that was allowed to stabilize for 30 min before imaging. Maximum intensity projections of Z-series stacks were analyzed using Image J software. Cell bodies and the ventral cord were outlined for each worm. In a given worm, the cell bodies and ventral cord sections were multiplied by the area that was outlined, and the values were summed and then divided by the total cell body or ventral cord area in order to obtain an average cell body or ventral cord fluorescent value for each worm. These average cell body and ventral cord fluorescent values were then averaged over nine worms for both the control (*unc-26(s1710); oxIs-92[GFP:UNC-26]*) and the mutant (*unc-57(ok310); unc-26(s1710); oxIs92*) strains. The quantitative analysis was performed independently by two individuals, one of which was given images that had been blinded. In each case the values obtained were virtually identical.

Acknowledgments

We thank D. Williams, S. Speese, and M. Bastiani for advice on fluorescent imaging and quantification. In addition, we thank the *C.*

elegans knockout consortium, the *C. elegans* Genetics Center, M. Nonet, A. Fire, Y. Kohara, A. Rowland, and M. Horner for reagents. We thank B. Bamber and W. Davis for critical reading of the manuscript. A.M.v.d.B. is supported by the National Institutes of Health (GM58166). D.A.R. is a recipient of a stipend from the NIH training grant T32-GM07104. This work was supported by NIH grants to J.E.R. and E.M.J., an ACS grant to D.S.M., and a grant from the Lowe Syndrome Association and the Lowe Syndrome Trust to K.R.S. and E.M.J.

Received: June 20, 2003
Revised: August 29, 2003
Accepted: September 17, 2003
Published: November 12, 2003

References

Balguerie, A., Sivadon, P., Bonneu, M., and Aigle, M. (1999). Rvs167p, the budding yeast homolog of amphiphysin, colocalizes with actin patches. J. Cell Sci. *112*, 2529–2537.

Bamber, B.A., Beg, A.A., Twyman, R.E., and Jorgensen, E.M. (1999). The *Caenorhabditis elegans* unc-49 locus encodes multiple subunits of a heteromultimeric GABA receptor. J. Neurosci. *19*, 5348–5359.

Clark, S.G., Lu, X., and Horvitz, H.R. (1994). The *Caenorhabditis elegans* locus *lin-15*, a negative regulator of a tyrosine kinase signaling pathway, encodes two different proteins. Genetics *137*, 987–997.

Cremona, O., Di Paolo, G., Wenk, M., Luthi, A., Kim, W.T., Takei, K., Daniell, L., Nemoto, Y., Shears, S.B., Flavell, R.A., et al. (1999). Essential role of phosphoinositide metabolism in synaptic vesicle recycling. Cell *99*, 179–188.

David, C., McPherson, P.S., Mundigl, O., and de Camilli, P. (1996). A role of amphiphysin in synaptic vesicle endocytosis suggested by its binding to dynamin in nerve terminals. Proc. Natl. Acad. Sci. USA *93*, 331–335.

De Camilli, P., Slepnev, V.I., Shupliakov, O., and Brodin, L. (2000). Synaptic vesicle endocytosis. In Synapses, W.M. Cowan, T.C. Sudhof, and C.F. Stevens, eds. (Baltimore, MD: The Johns Hopkins University Press), pp. 217–274.

de Heuvel, E., Bell, A.W., Ramjaun, A.R., Wong, K., Sossin, W.S., and McPherson, P.S. (1997). Identification of the major synaptojanin-binding proteins in the brain. J. Biol. Chem. *272*, 8710–8716.

Farsad, K., Ringstad, N., Takei, K., Floyd, S.R., Rose, K., and De Camilli, P. (2001). Generation of high curvature membranes mediated by direct endophilin bilayer interactions. J. Cell Biol. *155*, 193–200.

Gad, H., Ringstad, N., Low, P., Kjaerulff, O., Gustafsson, J., Wenk, M., Di Paolo, G., Nemoto, Y., Crun, J., Ellisman, M.H., et al. (2000). Fission and uncoating of synaptic clathrin-coated vesicles are perturbed by disruption of interactions with the SH3 domain of endophilin. Neuron *27*, 301–312.

Gaidarov, I., and Keen, J.H. (1999). Phosphoinositide-AP-2 interactions required for targeting to plasma membrane clathrin-coated pits. J. Cell Biol. *146*, 755–764.

Ge, K., and Prendergast, G.C. (2000). Bin2, a functionally nonredundant member of the BAR adaptor gene family. Genomics *67*, 210–220.

Guichet, A., Wucherpfenning, T., Dudu, V., Etter, S., Wilsch-Brauniger, M., Hellwig, A., Gonzalez-Gaitan, M., Huttner, W.B., and Schmid, S.L. (2002). Essential role of endophilin A in synaptic vesicle budding at the *Drosophila* neuromuscular junction. EMBO J. *21*, 1661–1672.

Hall, D.H., and Hedgecock, E.M. (1991). Kinesin-related gene *unc-104* is required for axonal transport of synaptic vesicles in *C. elegans*. Cell *65*, 837–847.

Hao, W., Tan, Z., Prasad, K., Reddy, K.K., Chen, J., Prestwich, G.D., Falck, J.R., Shears, S.B., and Lafer, E.M. (1997). Regulation of AP-3 function by inositides. Identification of phosphatidylinositol 3,4,5-trisphosphate as a potent ligand. J. Biol. Chem. *272*, 6393–6398.

Harris, T.W., Hartwieg, E., Horvitz, H.R., and Jorgensen, E.M. (2000). Mutations in synaptojanin disrupt synaptic vesicle recycling. J. Cell Biol. *150*, 589–600.

Harris, T.W., Schuske, K., and Jorgensen, E.M. (2001). Studies of synaptic vesicle endocytosis in the nematode *C. elegans*. Traffic *2*, 597–605.

Hill, E., van Der Kaay, J., Downes, C.P., and Smythe, E. (2001). The role of dynamin and its binding partners in coated pit invagination and scission. J. Cell Biol. *152*, 309–323.

Jorgensen, E.M., Hartwieg, E., Schuske, K., Nonet, M.L., Jin, Y., and Horvitz, H.R. (1995). Defective recycling of synaptic vesicles in synaptotagmin mutants of *Caenorhabditis elegans*. Nature *378*, 196–199.

Koenig, J.H., and Ikeda, K. (1989). Disappearance and reformation of synaptic vesicle membrane upon transmitter release observed under reversible blockage of membrane retrieval. J. Neurosci. *9*, 3844–3860.

Letunic, I., Goodstadt, L., Dickens, N.J., Doerks, T., Schultz, J., Mott, R., Ciccarelli, F., Copley, R.R., Ponting, C.P., and Bork, P. (2002). Recent improvements to the SMART domain-based sequence annotation resource. Nucleic Acids Res. *30*, 242–244.

McIntire, S.L., Reimer, R.J., Schuske, K., Edwards, R.H., and Jorgensen, E.M. (1997). Identification and characterization of the vesicular GABA transporter. Nature *389*, 870–876.

Micheva, K.D., Kay, B.K., and McPherson, P.S. (1997a). Synaptojanin forms two separate complexes in the nerve terminal. Interactions with endophilin and amphiphysin. J. Biol. Chem. *272*, 27239–27245.

Micheva, K.D., Ramjaun, A.R., Kay, B.K., and McPherson, P.S. (1997b). SH3 domain-dependent interactions of endophilin with amphiphysin. FEBS Lett. *414*, 308–312.

Miller, D.M., and Shakes, D.C. (1995). Immunofluorescence microscopy. Methods Cell Biol. *48*, 365–394.

Modregger, J., Schmidt, A., Ritter, B., Huttner, W.B., and Plomann, M. (2003). Characterization of endophilin B1b, a brain-specific membrane-associated lysophosphatidic acid acyl transferase with properties distinct from endophilin A1. J. Biol. Chem. *278*, 4160–4167.

Nonet, M.L., Staunton, J.E., Kilgard, M.P., Fergestad, T., Hartweig, E., Horvitz, H.R., and Jorgensen, E.M. (1997). *Caenorhabditis elegans* rab-3 mutant synapses exhibit impaired function and are partially depleted of vesicles. J. Neurosci. *17*, 8061–8073.

Nonet, M., Holgado, A.M., Brewer, F., Serpe, C.J., Norbeck, B.A., Holleran, J., Wei, L., Hartwieg, E., Jorgensen, E.M., and Alfonso, A. (1999). UNC-11, a *Caenorhabditis elegans* AP180 homologue, regulates the size and protein composition of synaptic vesicles. Mol. Biol. Cell *10*, 2343–2360.

Ringstad, N., Nemoto, Y., and De Camilli, P. (1997). The SH3p4/Sh3p8/SH3p13 protein family: binding partners for synaptojanin and dynamin via a Grb2-like Src homology 3 domain. Proc. Natl. Acad. Sci. USA *94*, 8569–8574.

Ringstad, N., Gad, H., Low, P., Di Paolo, G., Brodin, L., Shupliakov, O., and De Camilli, P. (1999). Endophilin/SH3p4 is required for the transition from early to late stages in clathrin-mediated synaptic vesicle endocytosis. Neuron *24*, 143–154.

Ringstad, N., Nemoto, Y., and DeCamilli, P. (2001). Differential expression of endophilin 1 and 2 dimers at central nervous system synapases. J. Biol. Chem. *276*, 40424–40430.

Schmidt, A., Wolde, M., Thiele, C., Fest, W., Kratzin, H., Podtelejnikov, A.V., Witke, W., Huttner, W.B., and Soling, H.D. (1999). Endophilin I mediates synaptic vesicle formation by transfer of arachidonate to lysophosphatidic acid. Nature *401*, 133–141.

Schultz, J., Milpetz, F., Bork, P., and Ponting, C. (1998). SMART, a simple modular architecture research tool: identification of signaling domains. Proc. Natl. Acad. Sci. USA *95*, 5857–5864.

Simpson, F., Hussain, N.K., Qualmann, B., Kelly, R.B., Kay, B.K., McPherson, P.S., and Schmid, S.L. (1999). SH3-domain-containing proteins function at distinct steps in clathrin-coated vesicle formation. Nat. Cell Biol. *1*, 119–124.

Slepnev, V.I., and De Camilli, P. (2000). Accessory factors in clathrin-dependent synaptic vesicle endocytosis. Nat. Rev. Neurosci. *3*, 161–172.

Tang, Y., Hu, L.A., Miller, W.E., Ringstad, N., Hall, R.A., Pitcher, J.A., DeCamilli, P., and Lefkowitz, R.J. (1999). Identification of the endophilins (SH3p4/p8/p13) as novel binding partners for the beta1-adrenergic receptor. Proc. Natl. Acad. Sci. USA *96*, 12559–12564.

Verstreken, P., Kjaerulff, O., Lloyd, T.E., Atkinson, R., Zhou, Y., Meinertzhagen, I.A., and Bellen, H.J. (2002). Endophilin mutations block clathrin-mediated endocytosis but not neurotransmitter release. Cell *109*, 101–112.

White, J.E., Southgate, E., Thomson, J.N., and Brenner, S. (1976). The structure of the ventral nerve cord of *C. elegans*. Philos. Trans. R. Soc. Lond. B Biol. Sci. *275*, 327–348.

Yook, K.J., Proulx, S.R., and Jorgensen, E.M. (2001). Rules of nonallelic noncomplementation at the synapse in *Caenorhabditis elegans*. Genetics *158*, 209–220.

Note Added in Proof

Verstreken et al. (this issue of *Neuron*) isolated *Drosophila* synaptojanin mutants and investigated the in vivo interaction between Synaptojanin and Endophilin. They found independently that a major role for Endophilin is to serve as an adaptor for Synaptojanin, stabilizing its expression at the synapse, thereby promoting vesicle uncoating. For further reading, see Verstreken, P., Koh, T.-W., Schulze, K.L., Zhai, R.G., Hiesinger, P.R., Zhou, Y., Mehta, S., Cao, Y., Roose, J., and Bellen, H.J. (2003). Synaptojanin is recruited by endophilin to promote synaptic vesicle uncoating. Neuron *40*, 733–748.